Ion dynamics in pendant and backbone polymerized ionic liquids:
A view from high-pressure dielectric experiments and free-volume model

Shinian Cheng [1,*] Zaneta Wojnarowska [1] Joshua Sangoro [2] and Marian Paluch[1]

[1]*Institute of Physics, University of Silesia in Katowice, Silesian Center for Education and Interdisciplinary Research,*
75 Pułku Piechoty 1A, 41–500 Chorzów, Poland

[2]*Department of Chemical and Biomolecular Engineering, University of Tennessee, Knoxville, Tennessee 37996, USA*

Polymerized ionic liquids (PILs) are typically single-ion conductors, where one kind of ionic species is either placed as the pendant group to the chain (pendant PILs) or directly incorporated into the polymeric backbone (backbone PILs). This paper compares the thermodynamics, ionic dynamics, and mechanical properties of pendant and backbone PILs. The results indicate that near the glass transition, the energy barrier for ion hopping is much lower for pendant PIL while the backbone PIL shows a much stronger sensitivity to pressure. At the same time, a free-volume based model was proposed here to understand the ion dynamics of both studied PILs at high-pressure conditions. The determined critical volume, quantifying the minimal volume required for ion hopping, of the pendant PIL is significantly reduced compared to the backbone PIL, which is most likely the reason for the enhanced ionic conductivity of the pendant PIL near the glass transition. We found that the proposed model is equivalent to the commonly used pressure counterpart of the Vogel-Fulcher-Tammann equation.

I. INTRODUCTION

Polymerization of ionic liquids results in the formation of poly(ionic liquid)s or polymerized ionic liquids (PILs) [1]. Combining the unique physical and chemical properties of low-molecular ionic liquids and outstanding mechanical stability of polymers, PILs exhibit many desired features, like high mechanical and thermal stability, low flammability, low vapor pressure, and wide electrochemical windows [2–4] that make them potential electrolytes in various electrochemical devices, such as batteries, supercapacitors, and fuel cells [5–7]. However, as one of the ionic species is covalently bonded to the polymer chain, PILs are essentially single-ion conductors and always exhibit a substantial decrease in the ionic conductivity compared to the monomeric ionic liquids. To serve as a viable solid-state alternative to traditional liquid electrolytes, PILs must be sufficiently conductive. An essential aspect of synthesizing highly conductive PILs for the design of advanced polymer electrolytes is to understand how polymer structure affects the charge transport and, thereby, ion conductivity. In standard synthetic methods, the ionic species can be either covalently bonded as a side chain (pendant group) or directly incorporated into the polymeric backbone, and therefore, PILs are commonly classified as pendant or backbone PILs, respectively.

It has been demonstrated that these two types of PILs exhibit significantly distinct ion dynamics. Runt *et al.* [8]. have compared a series of pendant and backbone PILs containing the same cation-anion pair. They found that the backbone PILs

exhibit higher conductivity at an absolute temperature scale, likely due to their relatively lower glass transition temperature T_g, while the pendant PILs show higher ionic conductivity when scaled to T_g, raising from the decoupling of ionic conductivity from structural dynamics. Sangoro *et al.* [9]. claimed that the unusually high mobility of free anions even near T_g might be responsible for such a decoupling. This view was further confirmed by Wojnarowska *et al.* [10]. based on the results of high-pressure dielectric measurements of another pendant imidazolium-based PIL. It has been shown that the decoupling between ion dynamics and segmental relaxation was reduced by squeezing the studied PIL due to the decrease in the free space available for motions of anions in the polymer matrix. Another high-pressure dielectric experiment and molecular dynamics simulations by Wojnarowska *et al.* [11]. have also demonstrated that chain rigidity of pendant PILs has significant effects on the decoupling of ion motion from segmental relaxation and free volume is a key quantity controlling such decoupling behavior. It has been indicated recently that the free volume also plays a significant role in governing the ion transport in a backbone PIL [12]. Actually, the free-volume theory originally proposed to interpret the structural dynamics of nonionic glass formers [13–15], has been applied multiple times to study the ionic conductivity of polymer electrolytes [16–18], like poly(ethylene oxide), and valuable information regarding the ion transport mechanism was gained. From this point of view, the free-volume theory might also be a powerful method to understand the ion transport mechanism in PILs. However, a systematic study of ion dynamics in pendant and backbone PILs on the basis of free-volume theory is still missing so far.

*shinian.cheng@smcebi.edu.pl

In the present work, the charge transport, structural dynamics, and thermodynamics of a backbone PIL: Poly(3-methyl-1,2,3-triazolium) bis(trifluoromethylsulfonyl)imide (TPIL) and a pendant PIL: Poly-1-vinyl-3-hexylimidazolium bis(trifuoromethylsulfonyl)imide (PHVI) are investigated by a combination of ambient and high-pressure dielectric spectroscopy, mechanical measurements, and differential scanning calorimetry. We find that the glass transition temperature of TPIL is around 75 K below that of PHVI, and the specific-heat capacity change at T_g of the former is around three times higher than the latter, indicating more thermal energy required for TPIL to transform from the glassy to the liquid state. Significant differences in ion dynamics of studied PILs are observed at ambient and elevated pressure conditions. Strong decoupling of ion transport from segmental dynamics is found in the studied pendant PIL, while coupling between these two processes is observed in the studied backbone PIL. A significant ionic conductivity, around 10^{-8} Scm^{-1}, is obtained in PHVI at T_g under ambient pressure conditions, which is six orders of magnitude higher than that of TPIL. A free-volume based model proposed here describes well the high-pressure ion dynamics of both studied PILs. Moreover, this model indicates that the critical volume, quantifying the minimal local free volume required for ion motion, of PHVI is reduced around 19% when compared to TPIL, which is most likely the reason for enhanced ionic conductivity of PHVI near the glassy state. Importantly, the proposed model is proven to be equivalent to the frequently used pressure counterpart of the Vogel-Fulcher-Tammann equation.

II. MATERIALS AND METHODS

A. Material

1. TPIL

TPIL was synthesized by the following three steps: (i) polyaddition of a triethylene glycol-based α-azide-ω-alkyne monomer by $AB + AB$ copper-catalyzed azide-alkyne cycloaddition; (ii) N-alkylation of the 1,2,3-triazole groups; and (iii) the introduction of the bis(trifluoromethylsulfonyl)imide (TFSI) counteranions using CH$_3$TFSI. More detailed information about the synthesis of TPIL can be found in Ref [19].

2. PHVI

PHVI was synthesized in two steps. All starting materials used for this synthesis (1-vinylimidazole, 1-iodohexane, t-butyl methyl ether) were distilled before use. A small excess of 1-iodohexane with respect to 1-vinyl imidazole (1.1 mole: 1mole) and 1-vinyl imidazole dissolved in t-butyl methyl ether were stirred under nitrogen at room temperature until the entire starting material was converted to 1-vinyl-3-hexyl imidazolium iodide (PHVIm I). Next, anion metathesis was conducted with lithium bis(trifluoromethylsulfonyl)imide to yield PHVIm TFSI (or PHVI). More information regarding the synthesis and characterization procedures is detailed in Ref. [9].

The chemical structures of studied PILs are presented below in Scheme 1. The two PILs have the same [TFSI]$^-$ anion.
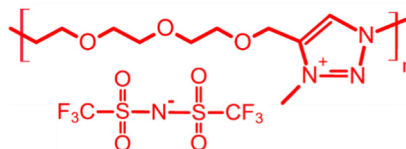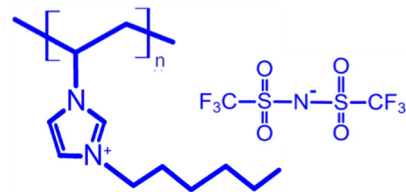
SCHEME 1. Chemical structures of studied PILs: (a) TPIL and (b) PHVI.

B. Methods

1. Differential scanning calorimetry

Differential scanning calorimetric (DSC) experiments of studied PILs were performed by a Mettler Toledo DSC1STAR System equipped with a liquid nitrogen cooling accessory and an HSS8 ceramic sensor with 120 thermocouples. The sample was measured in an aluminum crucible with the volume being equal to 40 μL. Prior to the measurement, the sample was annealed for 15 min at 373 K. During the experiments, the nitrogen flow was kept at 60 mLmin^{-1} and the heating rate was 10 Kmin^{-1}. Enthalpy and temperature calibrations were performed using indium and zinc standards.

2. Broadband dielectric spectroscopy measurements

The dielectric measurements at ambient pressure conditions were performed over a wide frequency range from 10^{-1} to 10^6 Hz by means of a Novocontrol Alpha High Resolution Dielectric Analyzer. The tested sample was placed between two round stainless-steel electrodes of the capacitor (diameter 10 mm) during the measurements. Teflon spacers with 100-μm diameter were used to ensure constant sample thickness. The temperature was controlled by the Novocontrol Quatro cryosystem with nitrogen gas cryostat. The temperature stability of the sample was better than 0.1 K. For the high-pressure dielectric measurements, the same capacitor was used. It was next insulated with Teflon tape and installed in a special holder. Then, such a prepared sealed cell was placed into the high-pressure chamber and compressed by a hydraulic pump using a nonpolar pressure-transmitting liquid (silicone oil). The pressure was measured with a resolution of 0.1 MPa. The temperature was controlled within 0.1 K by means of Weiss fridge.

3. Rheological measurements

The structural dynamics of PHVI were measured by using an ARES G2 Rheometer. An aluminum parallel-plates geometry with a diameter of 4 mm was applied to perform the shear modulus measurements. The studied PIL were investigated in the frequency range from 0.1 to 100 rad s^{-1} (12 points per decade) and over the temperature range from 316 to 383 K.

III. RESULTS AND DISCUSSION

The specific-heat capacity (c_p) of studied PILs at ambient pressure was determined from the DSC measurements. As shown in Fig. 1, for each studied ionic polymer, a pronounced steplike change in the $c_p(T)$ dependence is revealed, indicating the glass transition process. The corresponding glass transition temperature was determined as the midpoint of the c_p step. The obtained T_g^{DSC} values are 322 K for PHVI and 247 K for TPIL. The fact that $T_g^{PHVIM} > T_g^{TPIL}$ agrees with recent reports that the glass transition temperature of backbone PILs is much lower than the pendant PILs [20]. Herein, it is also interesting to calculate the heat capacity change at T_g, namely, $\Delta c_p(T_g) = c_p^{liquid}(T_g) - c_p^{glass}(T_g)$. The obtained $\Delta c_p(T_g)$ value of TPIL is 0.41 JK^{-1}g^{-1} which is around three times larger than that of PHVI, being 0.11 JK^{-1}g^{-1}. It indicates that much more energy is required for TPIL than PHVI to transform from the glassy to the liquid state.

To investigate the ion dynamic behavior of PHVI, we performed the dielectric measurements in the frequency domain from 253 to 393 K at 0.1 MPa. Since the studied sample is ion-conducting material, the complex conductivity $\sigma^*(f) = \sigma'(f) + i\sigma''(f)$ and electrical modulus $M^*(f) = M'(f) + iM''(f)$ formalisms were chosen to present the experimental data [21]. The representative dielectric spectra of PHVI are presented in Fig. 2.

As illustrated in Fig. 2, at each temperature, $\sigma'(f)$ reveals a visible frequency-independent plateau, corresponding to the DC conductivity (σ_{DC}). Moreover, due to the slowing down of ion mobility with cooling, the σ_{DC} values of PHVI decrease with lowering temperature. At the same time, in the frequency window, the imaginary part of the complex modulus reveals a well-pronounced peak, reflecting the conductivity relaxation. Therefore, the characteristic timescale of conductivity relaxation (τ_σ) can be determined from the frequency of M' peak maximum, namely, $\tau_\sigma = 1/(2\pi f_{max})$. The conductivity relaxation peak shifts to lower frequencies and longer relaxation time upon cooling.

To provide a detailed description of the ion dynamics of PHVI, the temperature evolutions of both σ_{DC} and τ_σ were determined by analyzing the $\sigma'(f)$ and $M'(f)$ spectra, respectively. At the same time, the σ_{DC} and τ_σ data of TPIL at

FIG. 2. The real part of the complex conductivity (a) and the imaginary part of the complex electric modulus (b) as functions of frequency at selected temperatures as indicated for PHVI at 0.1 MPa.

ambient pressure conditions were taken from Refs. [22,23]. As shown in Figs. 3(a) and 3(b), at a certain temperature, $\sigma_{DC}(T)$ or $\tau_\sigma(T)$ dependence reveals a clear transition from Vogel-Fulcher-Tammann (VFT) to Arrhenius behavior. It indicates a liquid-glass transition and the corresponding
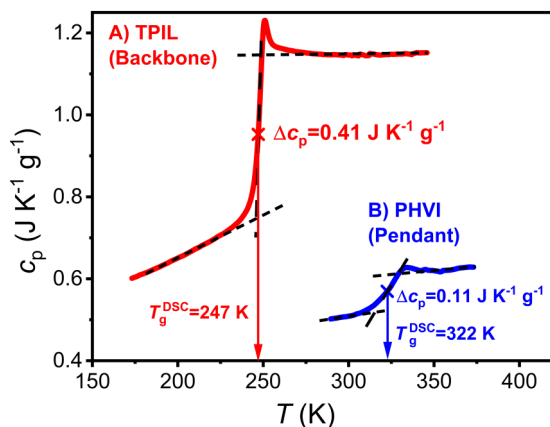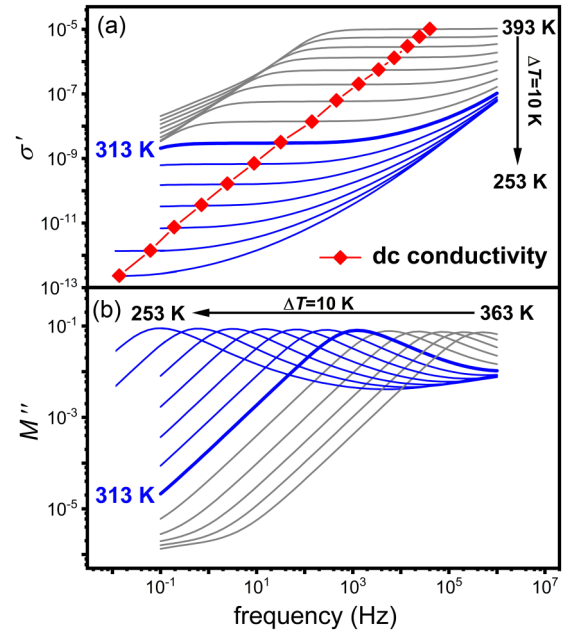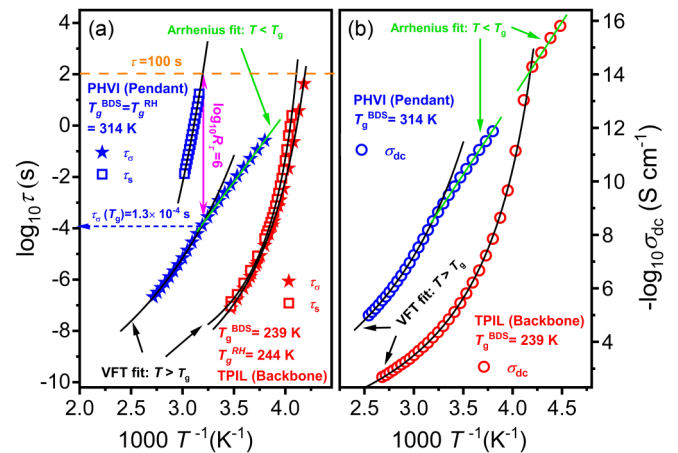
FIG. 1. The specific heat capacity of (a) TPIL and (b) PHVI at ambient pressure conditions determined from DSC.

FIG. 3. The temperature dependences of τ_σ, τ_s, and σ_{DC} for studied PILs. The data are parametrized by using VFT ($T > T_g$) and Arrhenius ($T < T_g$) equations. The determined VFT fitting parameters for PHVI are $\log_{10}\tau_{\sigma\infty} = -12.68 \pm 0.20$ s, $D_{VF} = 12.12 \pm 0.91$, $T_{VF} = 196.11 \pm 3.81$ K (τ_{sigma}); $\log_{10}\sigma_{DC\infty} = 0.29 \pm 0.13$ S cm^{-1}, $D_{VF} = 9.59 \pm 0.54$, $T_{VF} = 208.20 \pm 2.82$ K (σ_{DC}); $\log_{10}\tau_{s\infty} = -19.59 \pm 1.31$ s, $D_{VF} = 18.18 \pm 2.95$, $T_{VF} = 229.17 \pm 6.21$ K (τ_s); and for TPIL are $\log_{10}\tau_{\sigma\infty} = -12.19 \pm 0.17$ s, $D_{VF} = 4.28 \pm 0.18$, $T_{VF} = 211.04 \pm 0.76$ K (τ_σ); $\log_{10}\sigma_{DCc\infty} = 0.02 \pm 0.12$ S cm^{-1}, $D_{VF} = 4.80 \pm 0.20$, $T_{VF} = 208.41 \pm 0.99$ K (σ_{DC}); $\log_{10}\tau_{s\infty} = -10.54 \pm 0.14$ s, $D_{VF} = 2.37 \pm 0.10$, $T_{VF} = 225.05 \pm 0.59$ K (τ_s).

crossover temperature can be regarded as the glass transition temperature. The T_g values obtained in this way are denoted as T_g^{BDS}, being 314 K for PHVI and 239 K for TPIL, and BDS is defined as broadband dielectric spectroscopy. Thus, the T_g of TPIL (the backbone PIL) is 75 K lower than that of PHVI (the pendant PIL), which is consistent with the calorimetric experiments above.

To examine the structural dynamics of PHVI, rheological measurements were performed. The constructed master curve of $G''(f)$ and $G'(f)$ is shown in Supplemental Material, Fig. S1 [24]. The temperature dependence of segmental relaxation times $\tau_s(T)$, taken directly as $\tau_s = 1/2\pi f_{max}$ (f_{max} is the frequency of loss modulus maximum), is displayed in Fig. 3(a). The segmental relaxation times of TPIL were taken from Ref. [22]. As seen from this figure, at T_g the timescale of conductivity relaxation of PHVI is around six decades faster than the typical segmental relaxation time, $\tau_s = 100$s. It means a strong decoupling (with decoupling index [25,26] $\log_{10}R_\tau = 6$) of ionic conductivity from segmental dynamics in studied pendant PIL. Such pronounced decoupling behavior was also reported previously for other imidazolium-based pendant PILs [9,10]. On the other hand, one may find that in the case of another PIL studied here, the timescales of conductivity and segmental relaxation at the glass transition are equal to each other, indicating a coupling between these two physical processes. In other words, the ionic conductivity of TPIL is mainly controlled by the segmental dynamics.

To parametrize the temperature dependences of experimental dynamical data in the supercooled liquid state, we applied the VFT equation [27]:

$$\log_{10}X = \log_{10}X_\infty + \log_{10}e\frac{D_{VF}T_{VF}}{T - T_{VF}}, \quad (1)$$

where X denotes τ_σ, τ_s, or σ_{DC}^{-1}, and X_∞, D_{VF}, and T_{VF} (the "Vogel" temperature) are fitting parameters. The fitting functions are depicted as solid lines in Fig. 3. Since the temperature dependence of τ_s near T_g is known, we calculated the fragility parameter (m_p) by using the determined VFT fitting parameters. Namely,

$$m_p = \frac{\partial \log_{10}\tau_s}{\partial(T_g/T)}\bigg|_{T=T_g} = \log_{10}e\frac{D_{VF}T_{VF}T_g}{(T_g - T_{VF})^2} \quad (2)$$

Here, the glass transition temperature T_g was defined as T at which $\tau_s = 100$ s. The obtained m_p values are 123 and 104 for TPIL and PHVI, respectively. Furthermore, the temperature dependence of σ_{DC} (or τ_σ) data enables us to determine the activation energy (E_a), quantifying the energy barrier needed for ion hopping, by using the following equation:

$$E_a = \ln 10R\left(\frac{\partial \log_{10}\tau_\sigma(\text{or }\sigma_{DC}^{-1})}{\partial T^{-1}}\right) = RD_{VF}T_{VF}\left(\frac{T}{T - T_{VF}}\right)^2. \quad (3)$$

The calculated E_a values at T_g are 149 kJ mo l^{-1} for PHVI and 508 kJ mo l^{-1} for TPIL. Therefore, the energy barrier of ion hopping at the glass transition of studied backbone PIL is around three times higher than that of the pendant PIL.

On the other hand, the Arrhenius equation was applied to parametrize the conductivity data and determine the activation
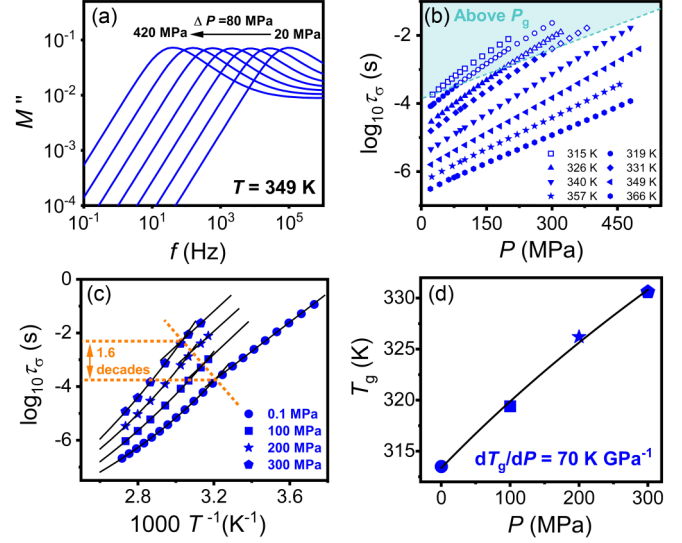

FIG. 4. (a) The representative $M'(f)$ spectra of PHVI from 20 to 420 MPa at $T = 349$ K; (b) τ_σ as a function of P at isothermal conditions; (c) The isobaric plots of $\log_{10}\tau_\sigma$ vs $1000T^{-1}$ at 0.1, 100, 200, and 300 MPa; (d) the plot of T_g as a function of P; the line denotes the fitting results by using the Anderson-Anderson equation.

energy in the glassy state:

$$\log_{10}\tau_\sigma\left(\text{or }\sigma_{DC}^{-1}\right) = \log_{10}\tau_\infty\left(\text{or }\sigma_\infty^{-1}\right) + \log_{10}e\frac{E_a}{RT}. \quad (4)$$

We found that the activation energy in the glassy state of studied PILs are the same and equal to 104 kJ mo l^{-1}, which is in good agreement with that reported by Sangoro *et al.* [28] on other imidazolium-based pendant PILs containing free [TFSI]$^-$ anions. Due to the substantial slowing down of polymer segments, free [TFSI]$^-$ anions dominate the glassy dynamics. Thus, $E_a = 104$ kJ mol^{-1} denotes the energy barrier required for hopping of free [TFSI]$^-$ anions. Herein, one should note that in the case of PHVI, the difference in activation energy at and below T_g is relatively small, while a significant decrease in E_a occurs for TPIL when it enters into the glassy state. This indicates that the segmental dynamics mainly controls the ionic conductivity of TPIL in the supercooled liquid state.

It has been envisioned that high-pressure dielectric studies can provide fundamental knowledge of the ion transport mechanism in polymerized ionic liquids [10,11,22,23,29]. For this reason, high-pressure dielectric measurements up to 500 MPa were performed on PHVI at several isothermal conditions. Since $\sigma'(f)$ and $M'(f)$ representations give the same information about ion dynamics, we chose the $M'(f)$ to present the high-pressure dielectric results of PHVI. The representative $M'(f)$ spectra of PHVI are shown in Fig. 4(a). One can see that the modulus loss peak moves to lower frequencies with compression, and thereby, the conductivity relaxation times become longer with an increase of pressure. Therefore, isothermal compression has the same effect on ion dynamics as isobaric cooling. The same as above, the conductivity relaxation times were determined as $\tau_s = 1/(2\pi f_{max})$ at each isotherm.

As illustrated in Fig. 4(b), the pressure dependence of τ_σ does not reveal a clear crossover to manifest the liquid-to-glass transition. Therefore, the liquid-glass transition pressure (P_g) cannot be determined directly from the $\tau_\sigma(P)$ dependences. For this reason, we plotted τ_σ as a function of $1000 \cdot T^{-1}$ at different isobaric conditions. As shown in Fig. 4(c), at each isobaric condition, the $\tau_\sigma(1000 \cdot T^{-1})$ dependence exhibits a departure from the VFT behavior, indicating a liquid-glass transition. Moreover, one may see that the conductivity relaxation times at T_g become longer when pressure increases. It indicates that the decoupling between segmental and conductivity relaxation in PHVI is reduced at high-pressure conditions. This result proves that the ion dynamics of PHVI is governed by mobility of the free [TFSI]$^-$ anions.

An important quantity reflecting the pressure sensitivity of glass transition temperature is the dT_g/dP coefficient determined in the limit of ambient pressure. To calculate it, we plotted T_g vs P, where T_g was defined as the crossover point of the isobaric $\tau_\sigma(1000 \cdot T^{-1})$ dependences presented in Fig. 4(c). The obtained $T_g(P)$ data of PHVI shown in Fig. 4(d) were subsequently analyzed by using the Anderson-Anderson equation [30]:

$$T_g(P) = k_1 \left(1 + \frac{k_2}{k_3}P\right)^{1/k_2}. \qquad (5)$$

The obtained value of $|dT_g/dP|_{P=0.1\,\text{MPa}}$ is equal to 70 KGP a^{-1}, which is much lower than that of TPIL [22,23], being 110 K GPa^{-1}. This indicates that the pressure sensitivity of PHVI is much weaker than that of TPIL.

Subsequently, the high-pressure dielectric data of examined PILs are analyzed through a free-volume based model, introduced by Duclot *et al.* in 2000 [31]. Based on the kinetic theory of ideal gas, they proposed the following expression of the free volume V_f:

$$V_f = \frac{R(T - T_0^*)}{P}, \qquad (6)$$

where $R = 8.314\,\text{J mo l}^{-1}\,\text{K}^{-1}$ is the gas constant, T_0^* is assumed as the "ideal" glass transition temperature at which the free volume would vanish, and T is the absolute temperature. Substituting the above equation into the classical free-volume model [15],

$$\sigma_{\text{DC}} \propto \exp\left(-\frac{V^*}{V_f}\right). \qquad (7)$$

Duclot *et al.* derived the following equation to describe the pressure dependence of DC conductivity at isothermal conditions:

$$\sigma_{\text{DC}} = \sigma_0 \exp\left[\frac{-PV^*}{R(T - T_0^*)}\right], \qquad (8)$$

where the per-exponential factor σ_0 denotes the DC conductivity in the limit of ambient pressure conditions and the critical volume V^* quantifies the minimal value of local free volume required for ion hopping. Moreover, Duclot *et al.* assumed that T_0^* is a pressure-independent parameter in the above equation. Since $\tau_\sigma \propto \sigma_{\text{DC}}^{-1}$, one can easily obtain the
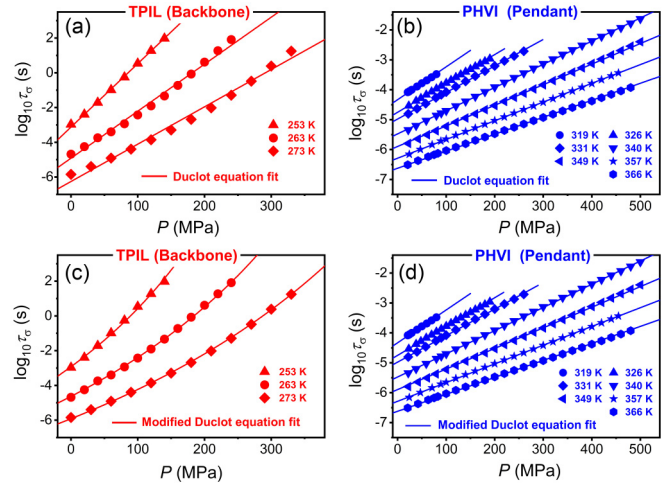

FIG. 5. The isothermal $\log_{10}\tau_\sigma(P)$ data of studied PILs are parametrized by using Duclot equation [(a), (b)] and modified Duclot equation [(c), (d)], respectively.

expression of τ_σ as a function of P:

$$\log_{10}\tau_\sigma = \log_{10}\tau_0 + \log_{10}e\,\frac{PV^*}{R(T - T_0^*)}. \qquad (9)$$

Here, τ_0 denotes the conductivity relaxation times in the limit of ambient pressure conditions and thereby reveals strong temperature dependence. In Figs. 5(a) and 5(b), we present the results of fitting Eq. (9) to the experimental isothermal $\tau_\sigma(P)$ data recorded in the supercooled liquid state of both studied PILs. One can see from Fig. 5(b) that the Duclot equation successfully describes the experimental $\tau_\sigma(P)$ data of PHVI with the obtained parameters being $V^* = 10.6 \pm 0.1\,\text{cm}^3\,\text{mol}^{-1}$ and $T_0^* = 268.7 \pm 1.0\,\text{K}$. It should be noted that the T_0^* determined here is much higher than $T_{\text{VF}} = 196.1 \pm 3.8\,\text{K}$. Thus, Duclot's assumption that $T_0^* \approx T_{\text{VF}}$ is not satisfied for the studied ionic polymer. On the other hand, we found that the Duclot equation cannot describe the experimental $\tau_\sigma(P)$ data of TPIL as shown in Fig. 5(a). It confirms that the Duclot equation fails to provide a general description of the high-pressure ion dynamics of PILs. The reason is likely due to the assumption of constant T_0^*. One may note that when T_0^* is a constant parameter, the Duclot equation captures a simple linear $\log_{10}\tau_\sigma(P)$ dependence at isothermal conditions and thereby fails to parametrize the nonlinear $\log_{10}\tau_\sigma(P)$ data of TPIL.

Actually, it has been reported by other authors that the "ideal" glass transition temperature T_0^* could change with pressure. For example, Cohen and Turnbull [32] have proposed the following linear dependence of T_0^* on P:

$$T_0^*(P) = T_0 + \alpha P. \qquad (10)$$

Here T_0 denotes the ideal glass transition temperature in the limit of ambient pressure and α is a constant parameter with the dimension of K GPa^{-1}. By applying this linear relation, we obtained the following modified Duclot equation:

$$\log_{10}\tau_\sigma = \log_{10}\tau_0 + \log_{10}e\,\frac{PV^*}{R(T - T_0 - \alpha P)}. \qquad (11)$$

TABLE I. The fundamental parameters of studied PILs.

	T_g K	T_{VF} K	T_0 K	$\Delta c_p(T_g)$ J K^{-1} g^{-1}	dT_g/dP K GPa^{-1}	$E_a(T_g)$ kJ mol^{-1}	E_a^{glass} kJ mol^{-1}	V^* cm^3 mol^{-1}	m_p
PHVI	322[DSC] 314[BDS] 314[RH]	196.1	268.7	0.11	70	149	104	10.6	104
TPIL	247[DSC] 239[BDS] 244[RH]	211.0	228.9	0.41	110	508	104	13.0	123

To test it, we reanalyzed the experimental $\tau_\sigma(P)$ data of studied PILs by Eq. (11). As shown in Figs. 5(c) and 5(d), the determined fitting curves are in good agreement with the experimental data for both studied PILs presenting different ion transport mechanisms. The determined parameters are the following (see Table I): $V^* = 10.6 \pm 0.2$ cm^3 mol^{-1}, $T_0 = 268.7 \pm 1.0$ K, and $a = 0.4 \pm 1.0$ K GPa^{-1} (PHVI) and $V^* = 13.0 \pm 0.4$ cm^3 mol^{-1}, $T_0 = 228.9 \pm 0.6$ K, and $a = 39.1 \pm 1.9$ KGPa^{-1} (TPIL). Herein, it should be noted that in the case of PHVI, the determined V^* and T_0 values are almost the same as those determined by the original Duclot equation. In addition, the obtained α value is quite close to zero, indicating that the ideal glass transition temperature T_0^* of PHVI is approximately independent of pressure. On the other hand, the obtained α value of TPIL is around two orders higher than that of PHVI, indicating that the former is much more sensitive to pressure than the latter. Moreover, we found that T_0 determined for TPIL is also higher than the T_{VF}. Specifically, the difference of $T_0 - T_{VF}$ is equal to 17.9 K for TPIL and becomes significantly lower than that found for PHVI (72.6 K). Notably, the critical volume V^* determined for PHVI is around 19% lower than that of TPIL, which indicates less free space required for ion transport in pendant PIL. This may be the reason why significant decoupling is observed in PHVI when approaching the glassy state.

Another interesting aspect is that the modified Duclot equation captures the same form of the commonly used pressure counterpart of the VFT (P-VFT) equation, namely,

$$\tau_\sigma = \tau_0 \exp\left[\frac{PV^*}{R(T - T_0 - \alpha P)}\right] = \tau_0 \exp\left[\frac{(V^*/\alpha R)P}{(T - T_0)/\alpha - P}\right]$$

$$= \tau_0 \exp\left[\frac{CP}{P_0(T) - P}\right], \tag{12}$$

with $C = V^*/(\alpha R)$ and $P_0(T) = (T - T_0)/\alpha$. Thus, a theoretical background of the empirical P-VFT formula may be found. According to these relations, one could assume that the parameter C in the P-VFT equation should be a material constant because V^* and α are constant parameters for a given system.

IV. CONCLUSION

In summary, the thermodynamics, ionic dynamics, and mechanical properties of a pendant PIL (PHVI) and a backbone PIL (TPIL) were studied through calorimetric, dielectric, and rheological experiments. The specific-heat capacity determined in the glass transition temperature region indicates that the energy barrier required for the glass transition of studied backbone PIL is significantly higher than that of the pendant PIL. The temperature dependences of conductivity and segmental relaxation times near T_g demonstrate that the ionic conductivity of the pendant PIL is decoupled from the segmental dynamics, while the segmental dynamics mainly control the conductivity relaxation of the backbone PIL. At the same time, we found that the isothermal τ_σ data of studied PILs obtained in high-pressure dielectric experiments also reveal different pressure sensitivity. An exponential increase of τ_σ with pressure is observed in the studied pendant PIL, while in case of the backbone PIL, the change of τ_σ with pressure is much faster than the exponential increase. These results indicate that the backbone PIL shows much higher sensitivity to pressure than the pendant PIL, which is also confirmed by dT_g/dP coefficient. Furthermore, we found that the Duclot equation properly describes only the experimental $\tau_\sigma(P)$ data of pendant PIL, i.e., where the ion dynamics is weakly sensitive to pressure. However, when improved by introducing a simple linear $T_0(P)$ dependence, the Duclot formula can describe well the experimental data of both studied PILs. Moreover, the improved model indicates that the significantly enhanced ionic conductivity of PHVI observed near the glass transition might be attributed to the relatively low critical volume for ion hopping. Finally, we proved that this proposed model is equivalent to the frequently used empirical P-VFT formula.

[1] A. Eftekhari and T. Saito, Synthesis and properties of polymerized ionic liquids, Eur. Polym. J. **90**, 245 (2017).

[2] D. Mecerreyes, Polymeric ionic liquids: Broadening the properties and applications of polyelectrolytes, Prog. Polym. Sci. **36**, 1629 (2011).

[3] W. Qian, J. Texter, and F. Yan, Frontiers in poly (ionic liquid) s: Syntheses and applications, Chem. Soc. Rev. **46**, 1124 (2017).

[4] N. Nishimura and H. Ohno, 15th anniversary of polymerised ionic liquids, Polymer **55**, 3289 (2014).

[5] M. Armand, F. Endres, D. R. MacFarlane, H. Ohno, and B. Scrosati, Ionic-liquid materials for the electrochemical challenges of the future, Nat. Mater. **8**, 621 (2009).

[6] T. Y. Kim, H. W. Lee, M. Stoller, D. R. Dreyer, C. W. Bielawski, R. S. Ruoff, and K. S. Suh, High-performance supercapacitors based on poly (ionic liquid)-modified graphene electrodes, ACS Nano **5**, 436 (2011).

[7] R. L. Weber, Y. Ye, A. L. Schmitt, S. M. Banik, Y. A. Elabd, and M. K. Mahanthappa, Effect of nanoscale morphology on the conductivity of polymerized ionic liquid block copolymers, Macromolecules **44**, 5727 (2011).

[8] P. Kuray, T. Noda, A. Matsumoto, C. Iacob, T. Inoue, M. A. Hickner, and J. Runt, Ion transport in pendant and backbone polymerized ionic liquids, Macromolecules **52**, 6438 (2019).

[9] J. R. Sangoro, C. Iacob, A. L. Agapov, Y. Wang, S. Berdzinski, H. Rexhausen, V. Strehmel, C. Friedrich, A. P. Sokolov, and F. Kremer, Decoupling of ionic conductivity from structural dynamics in polymerized ionic liquids, Soft Matter **10**, 3536 (2014).

[10] Z. Wojnarowska, J. Knapik, J. Jacquemin, S. Berdzinski, V. Strehmel, J. R. Sangoro, and M. Paluch, Effect of pressure on decoupling of ionic conductivity from segmental dynamics in polymerized ionic liquids, Macromolecules **48**, 8660 (2015).

[11] Z. Wojnarowska, H. Feng, Y. Fu, S. Cheng, B. Carroll, R. Kumar, V. N. Novikov, A. M. Kisliuk, T. Saito, N.-G. Kang *et al.*, Effect of chain rigidity on the decoupling of ion motion from segmental relaxation in polymerized ionic liquids: Ambient and elevated pressure studies, Macromolecules **50**, 6710 (2017).

[12] S. Cheng, Z. Wojnarowska, M. Musiał, S. Kolodziej, E. Drockenmuller, and M. Paluch, Studies on ion dynamics of polymerized ionic liquids through the free volume theory, Polymer **212**, 123286 (2021).

[13] A. K. Doolittle, Studies in Newtonian flow. II. The dependence of the viscosity of liquids on free-space, J. Appl. Phys. **22**, 1471 (1951).

[14] M. H. Cohen and D. Turnbull, Molecular transport in liquids and glasses, J. Chem. Phys. **31**, 1164 (1959).

[15] D. Turnbull and M. H. Cohen, Free-volume model of the amorphous phase: Glass transition, J. Chem. Phys. **34**, 120 (1961).

[16] S. J. Pas, M. D. Ingram, K. Funke, and A. J. Hill, Free volume and conductivity in polymer electrolytes, Electrochim. Acta **50**, 3955 (2005).

[17] D. Bamford, A. Reiche, G. Dlubek, F. Alloin, J. Y. Sanchez, and M. A. Alam, Ionic conductivity, glass transition, and local free volume in poly (ethylene oxide) electrolytes: Single and mixed ion conductors, J. Chem. Phys. **118**, 9420 (2003).

[18] A. Reiche, G. Dlubek, A. Weinkauf, B. Sandner, H. M. Fretwell, A. A. Alam, G. Fleischer, F. Rittig, J. Kärger, and W. Meyer, Local free volume and structure of polymer gel

[19] B. P. Mudraboyina, M. M. Obadia, I. Allaoua, R. Sood, A. Serghei, and E. Drockenmuller, 1,2,3-Triazolium-based poly(ionic liquid)s with enhanced ion conducting properties obtained through a click chemistry polyaddition strategy, Chem. Mater. **26**, 1720 (2014).

[20] V. Bocharova, Z. Wojnarowska, P. F. Cao, Y. Fu, R. Kumar, B. Li, V. N. Novikov, S. Zhao, A. Kisliuk, T. Saito, and J. W. Mays, Influence of chain rigidity and dielectric constant on the glass transition temperature in polymerized ionic liquids, J. Phys. Chem. B **121**, 11511 (2017).

[21] F. Kremer and A. Schoenhals, *Broadband Dielectric Spectroscopy* (Springer, Berlin, 2003).

[22] Z. Wojnarowska, M. Musiał, S. Cheng, E. Drockenmuller, and M. Paluch, Fast secondary dynamics for enhanced charge transport in polymerized ionic liquids, Phys. Rev. E **101**, 032606 (2020).

[23] S. Cheng, Z. Wojnarowska, M. Musiał, D. Flachard, E. Drockenmuller, and M. Paluch, Access to thermodynamic and viscoelastic properties of poly (ionic liquid) s using high-pressure conductivity measurements, ACS Macro Lett. **8**, 996 (2019).

[24] See Supplemental Material at http://link.aps.org/supplemental/10.1103/PhysRevE.105.054502 for the constructed master curve of G"(f) and G'(f) of PHVI.

[25] C. A. Angell, Fast ion motion in glassy and amorphous materials, Solid State Ionics **9**, 3 (1983).

[26] M. D. Ingram and C. T. Imrie, New insights from variable-temperature and variable-pressure studies into coupling and decoupling processes for ion transport in polymer electrolytes and glasses, Solid State Ionics **196**, 9 (2011).

[27] H. Vogel, Das Temperaturabhängigkeitsgesetz der Viskosität von Flüssigkeiten, Phys. Z. **22**, 645 (1921); G. S. Fulcher, Analysis of recent measurements of the viscosity of glasses, J. Am. Ceram. Soc. **8**, 339 (1925); G. Tamman and W. Hesse, Die Abhängigkeit der Viskosität von der Temperatur bei unterkühlten Flüssigkeiten, Z. Anorg. Allg. Chem. **156**, 245 (1926).

[28] M. Heres, T. Cosby, E. U. Mapesa, H. Liu, S. Berdzinski, V. Strehmel, M. Dadmun, S. J. Paddison, and J. Sangoro, Ion transport in glassy polymerized ionic liquids: Unraveling the impact of the molecular structure, Macromolecules **52**, 88 (2018).

[29] Z. Wojnarowska, H. Feng, M. Diaz, A. Ortiz, I. Ortiz, J. Knapik-Kowalczuk, M. Vilas, P. Verdia, E. Tojo, T. Saito *et al.*, Revealing the charge transport mechanism in polymerized ionic liquids: Insight from high pressure conductivity studies, Chem. Mater. **29**, 8082 (2017).

[30] S. P. Andersson and O. Andersson, Relaxation studies of poly (propylene glycol) under high pressure, Macromolecules **31**, 2999 (1998).

[31] M. Duclot, F. Alloin, O. Brylev, J. Y. Sanchez, and J. L. Souquet, New alkali ionomers: Transport mechanism from temperature and pressure conductivity measurements, Solid State Ionics **136**, 1153 (2000).

[32] M. H. Cohen and G. S. Grest, Liquid-glass transition, a free-volume approach, Phys. Rev. B **20**, 1077 (1979).